# Innovative High Pressure Vessel Seal design and Optimisation

Slee A.J[1,2,3], Hardy S.J[2], Gethin D.T[2], Stobbart J[3], Miot S[4]

[1] STRIP Project, Unit 20, Baglan Bay Innovation Centre, Baglan Energy Park, SA12 7AX, UK
[2] College of Engineering, Swansea University, Singleton Park, Swansea, SA2 8PP, UK
[3]Vector Technology Group, Unit 18, Baglan Industrial Estate, Port Talbot, SA12 7BY, UK
[4]SSA, Southill Barn, Southhill Business Park, Charlbury, Oxfordshire, OX7 3EW, UK

***Abstract***: *The results from a project to investigate the design & optimisation of a metallic seal ring as part of an end cap for a 140 tonne pressure vessel are presented. A vessel loading condition of 4483 bar (65,000 psi) internal pressure was stipulated. The design of a metallic seal of 762 mm (30") bore diameter provided a challenging task, due to the extremely high pressure application.*

*A detailed Finite Element Analysis (FEA) was carried out to evaluate the seal and the initial conclusion was that it required complete re-design. In this work, analysis and interpretation was used to establish the modelling method for the seal. The FEA model that was developed for seal optimisation contained elasto-plastic material response, frictional contact modelling, advanced pressure field application and thermal modelling.*

*To maintain sealing contact pressure, the seal has to overcome differential radial movement between the vessel and the end cap during pressure loading. The optimisation process developed a novel profiled seal contact that reduced contact stresses by 48%, eliminating seat damage occurring during pressure loadings.*

*Structural deformations cause the seal contact point to shift, providing the opportunity for liquid to penetrate up to the contact point. Limitations were recognised within the FE software, which allowed unidirectional pressure penetration only. To overcome this limitation, a bespoke user subroutine was written to revise the contact algorithms within the Abaqus FE program. This enabled 'contact pressure zones' to correctly progress and (for the first time) regress in real time, with seal and seat movements.*

***Keywords***: *Assembly Deformation, Bolt Loading, Design Optimization, Heat Transfer, Interface Friction, Low-Cycle Fatigue, Model Verification, Optimization, Plasticity, Pressure Penetration, Pressure Vessel, Metallic Seal, User Subroutine, Shrink Fit.*

## 1. Introduction

This paper contains the results of two separate interconnected analyses which use Abaqus/Standard (6.12-3) FEA software to solve two complex problems. The two sections in this paper cover the analysis of a seal ring in an extremely high pressure vessel (Figure 1-1) and the production of a unique user subroutine which allows accurate pressure field application.

The pressure vessel analysis is focused on a pressure energised metallic seal ring. These types of seals are used to maintain high integrity seal characteristics at extremely high pressures. At such extreme pressure however, the energisation force can be sufficient to damage the seal seats by indentation. The challenge therefore for this work was to ensure suitable contact was maintained from zero to 65,000 psi vessel pressure, whilst causing no seat damage and having the flexibility to accommodate different flexural characteristics of the mating parts.

The aim was to create a very accurate model of the entire vessel assembly. This would ensure accurate movement prediction of the individual components and therefore would allow effective optimisation. The approach that has been adopted is one of 'optimisation through inspection and interpretation' rather than exploiting a formal numerical approach.

Figure 1-1 summarises the problem. The end cap (blind) (1) is held down by 12 fixing bolts (5,8) and so only a 15 degree wedge needs to be analysed when symmetry through the bolt is exploited. The vessel (4) is made from a low alloy steel and a liner (3) is fitted within to provide the appropriate corrosion protection. The blind (1) features a rotation stop (6) that constrains the deformation of the blind itself. The assembly comprises a number of interfaces at which contact models are required. The formal treatment of these contacts and how they open and close when subjected to high pressure and their impact on the seal (2) is the thrust of this paper.

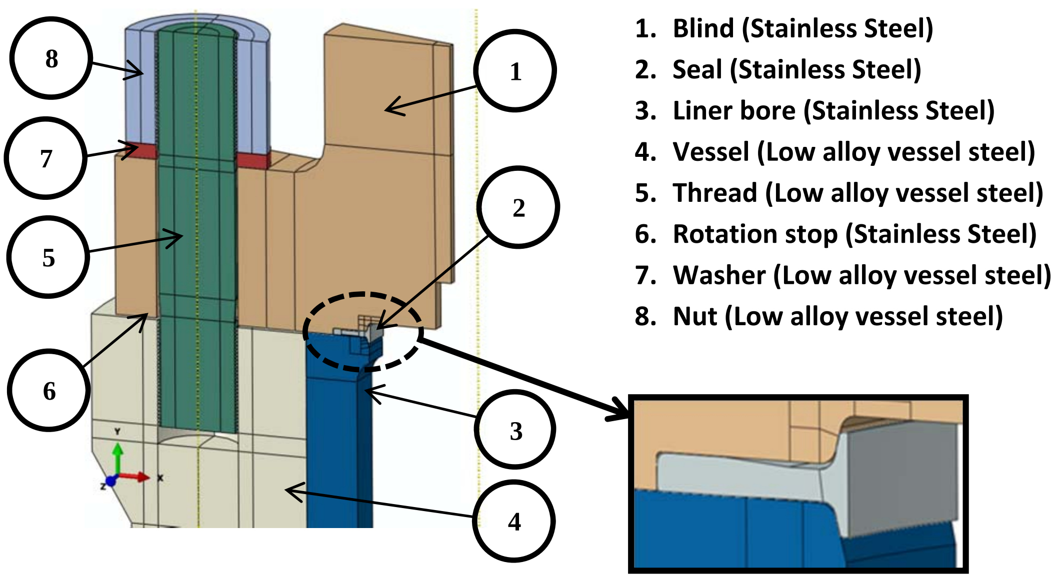


**Figure 1-1: Pressure vessel layout**

## 2. Notation

In this paper, the following notation has been used (Table 2-1).

**Table 2-1: Notation**

| Abbreviation | Description |
|---|---|
| **psi** | Pounds per square inch |
| **in** | Inches |
| **bar** | Pressure |
| **°F** | Degrees Fahrenheit |
| **Ibf/in$^2$** | Young's Modulus |
| **LPF** | Load percentage factor |
| **URDFIL** | Subroutine to access results data |
| **DLOAD** | Subroutine to specify loading parameters |
| **UVARM** | Subroutine to plot loadings as contour |

## 3. Pressure Vessel Modelling

### 3.1 Model Layout and Setup

All model geometry was developed within Solidworks Standard (2011) and imported as a 3D solid using an ACIS SAT format. The modelled assembly is laid out as shown in Figure 1-1.

Because the analysis is focused on a steady state application an implicit solution scheme was used. Simulation steps were created within Abaqus to firstly allow convergence of the model and secondly allow predictions to be easily viewed. This also displays how the model is reacting at each stage in the assembly/pressurization sequence. The steps created are shown in Figure 3-1:-

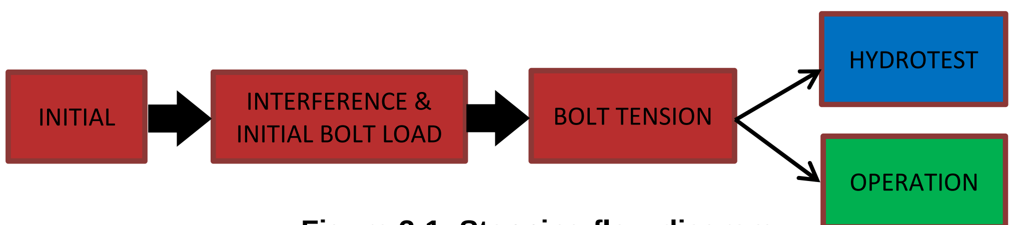


**Figure 3-1: Stepping flow diagram**

where:

**Initial** state sets up boundary conditions that include symmetry constraints and the edge constraints required to avoid solution singularity (i.e. a flying structure).

**Interference & initial bolt load** step computes the interference between the vessel and liner, activates all of the defined contacts (with contact control) whilst applying a very low initial bolt load of 100 pounds; this is to bring the contacts together.

**Bolt tension** step applies the full 52,000 psi bolt load using the same contact stabilisation method as above. The bolt loading is linearly ramped up to 0.5% at 0.5 Load Percentage Factor (LPF), then it reaches 100% bolt load at 1 LPF; this is to help the contacts converge.

**Hydrotest** loading is where the pressure vessel is linearly cycled between 0 psi, 65,000 psi, 32,500 psi, 63,700 psi and back to 0 psi.

**Operation** step applies both internal pressure and static thermal loadings to the designated areas. The pressure/temperature cycles in a linear fashion from 0 psi at 0 °F, up to 32,500 psi at 500 °F.

### 3.2 Material Modelling

Two types of material modelling are incorporated within the simulation material database, these are elastic and plastic. The von Mises stress predictions dictate what regions would be set as either elastic or plastic; however a plastic specified region would take longer to converge, so being conservative with the application of material zones is important. Preliminary elastic only investigations were performed to dictate what regions should be plastic. Three different materials regions were specified and applied to the assembly parts as required these also contain thermal expansion coefficients. Shown as an example in Figure 3-2 is a plot of three material data sets for each temperature case, where it was considered to be conservative with the yield points and extract these values once the data moves beyond the elastic limit. The yield values were 91552 psi at 100°F, 72623 psi at 300 °F and 67353 psi at 550°F. If these values were taken at 0.2% proof stress, it would have reduced the accuracy of the results, so the values used would be classed as the worst case scenario.

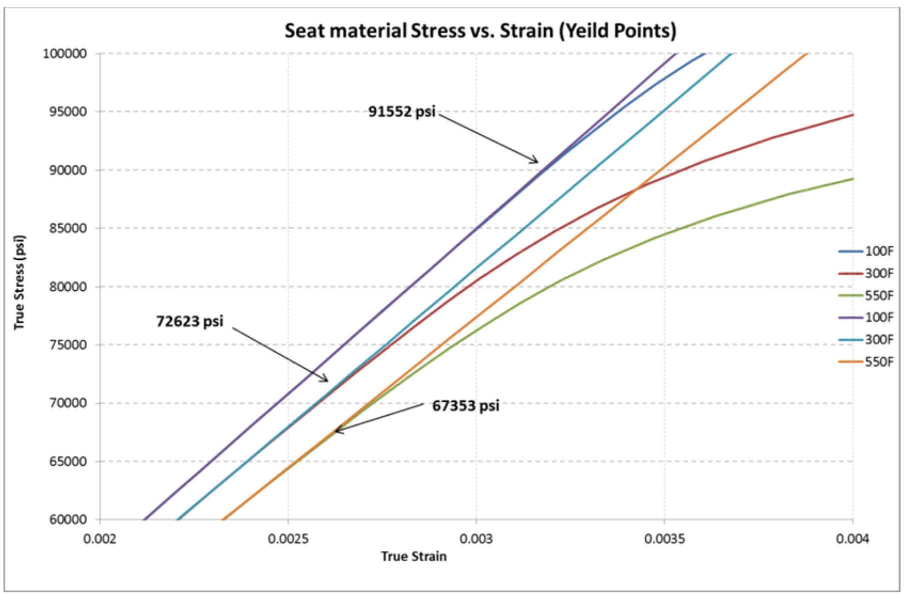


**Figure 3-2: Seat material characteristics**

Secondly the correct type of hardening model needs to be taken into account. The kinematic hardening model is for cyclic loading. Unsymmetrical cycles of stress between prescribed limits will cause progressive "ratcheting" in the direction of mean stress. Ratcheting is the progressive increase in strain at each cycle. The Bauschinger effect within an uniaxial test yields the material, then unloading occurs which continues so that yield occurs in the opposite direction; the yield stress is now reduced (the yield locus is shifted) compared to the original specimen when the material is compressed [1].

Due to seal rings being single use, it was not necessary to extend material characterisation to implement a kinematic material model within the FEA. No ratchetting occurred during operational cycles (32,500 psi) as the seal undergoes minimal plastic strain during pressurisation. Thus the material model did not include any Bauschiner effects, but where there is a cyclic pressurisation is simulated, the Bauschiner effect will need to be included.

### 3.3 FEA Model Verification

When the liner is shrunk fit into the vessel, it is necessary to verify that the model setup was correct and that the cylindrical coordinate system and interactions were working as desired. To perform this, a model was created solving the interference of 0.025” radially between the two components using friction coefficients to mimic a rough surface due to Poisson effects leading to relative movement between the liner and its case. The contact pressures and deflections were then compared to theoretical calculations. The section of interest (4 nodes in line) is shown in Figure 3-3.

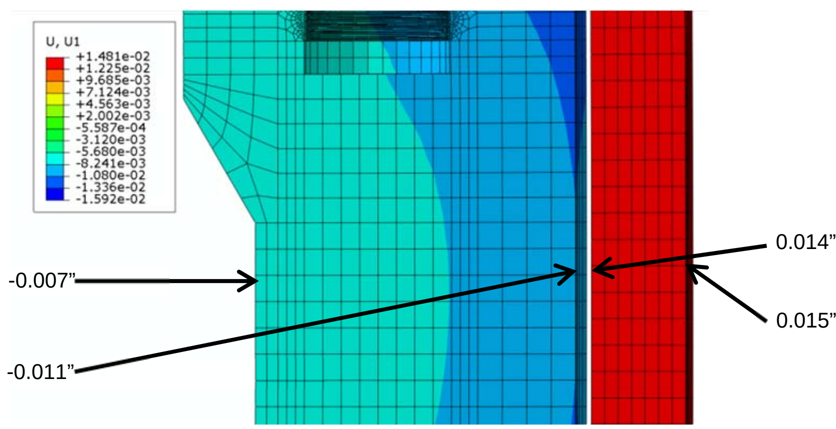


**Figure 3-3: Vessel to liner deflections**

The results were compared with calculations from thick cylinder theory [2] and these are itemised in Table 2-1 showing excellent agreement. The material and geometry data used for the calculations are shown in Table 3-2, and this data was also used in the FEA model.

**Table 3-1: FEA back check discrepancy**

| | Calculation | FEA result | Discrepancy (%) |
|---|---|---|---|
| **Inner Liner Wall (U1)** | 0.015” | 0.015” | 0 |
| **Outer Liner (U1)** | 0.0143” | 0.014” | 2 |
| **Inner Vessel Wall (U1)** | -0.0107” | -0.011” | 3 |
| **Outer Vessel Wall (U1)** | -0.0072” | -0.007” | 3 |
| **Interference Pressure (psi)** | 6382 | 6345 | 0.6 |

**Table 3-2: Thick cylinder material data**

| | Units | Value |
|---|---|---|
| **Young’s Modulus (liner)** | $Ibf/in^2$ | 28338000 |
| **Young’s Modulus (vessel)** | $Ibf/in^2$ | 27638000 |
| **Poisson’s Ratio** | - | 0.3 |
| **Radial Interference** | in | 0.025 |
| **Internal radius of liner** | in | 16.7475 |
| **Outer radius of liner** | in | 23.775 |
| **Outer radius of vessel** | in | 48 |

All results shown here are very promising with the largest discrepancy being 3%. Furthermore, when looking at the difference between the ‘outer liner’ and ‘inner vessel’ deflections, these result in 0.025” for both the FEA and thick cylinder theory work; confirming accuracy, as the interference was set at 0.025”.

### 3.4 Proposed Seal Ring Model

The proposed seal ring utilised a standard conical type sealing interface. The pressure loadings were applied to the entire internal surfaces of the reactor, where any end thrusts due to vessel ports were applied to their relevant faces and expressed as a pressure. With regards to the seal ring, the pressure loading was applied (statically) up to the seal interface as shown in Figure 3-4 (red outline).

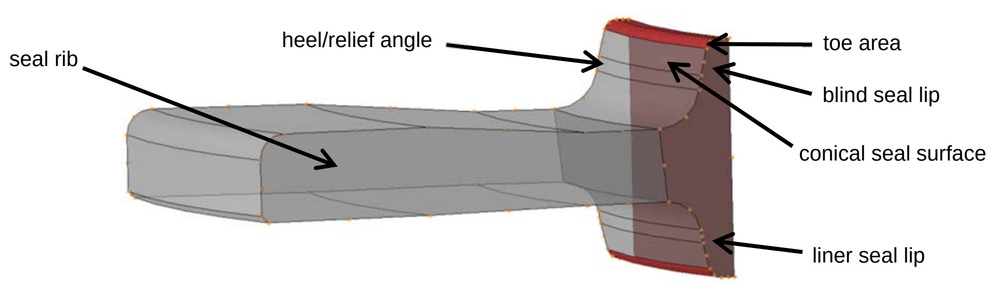


**Figure 3-4: Seal pressure load location**

A secondary method was also implemented in more recent models, where a module within Abaqus called ‘pressure penetration’ allows contact pressure tracking, pressure field application; this should accurately represent what occurs within the reactor with regards to loading position.

To capture localised stress transfer between seal and seat contact, a dense seat mesh was specified in the contact area for this model; if this change is not implemented the seal’s localised stresses will not be translated across the contact correctly and the seat integration points will result in ‘contact stress averaging’ and give lower resultant stresses.

The simulation for this particular seal design (Figure 3-4) was run using the hydrotest pressure loading case. A contact pressure plot of the seal at full 65,000 psi bore pressure is shown in Figure 3-6, where the following can be observed:

- Maximum make-up contact stresses are quite acceptable (above 1.8) with respect to the bore to CPRESS ratio (Figure 3-5); however the area utilised is a very narrow band. Further work would require decreasing this maximum CPRESS value.
- Maximum contact stresses (Figure 3-5) are reaching a very high 280,000 psi due to the geometry and this is why the pressure to CPRESS ratio is well above the target limit (1.8), however the contact area and position used is not acceptable; see Figure 3-6.

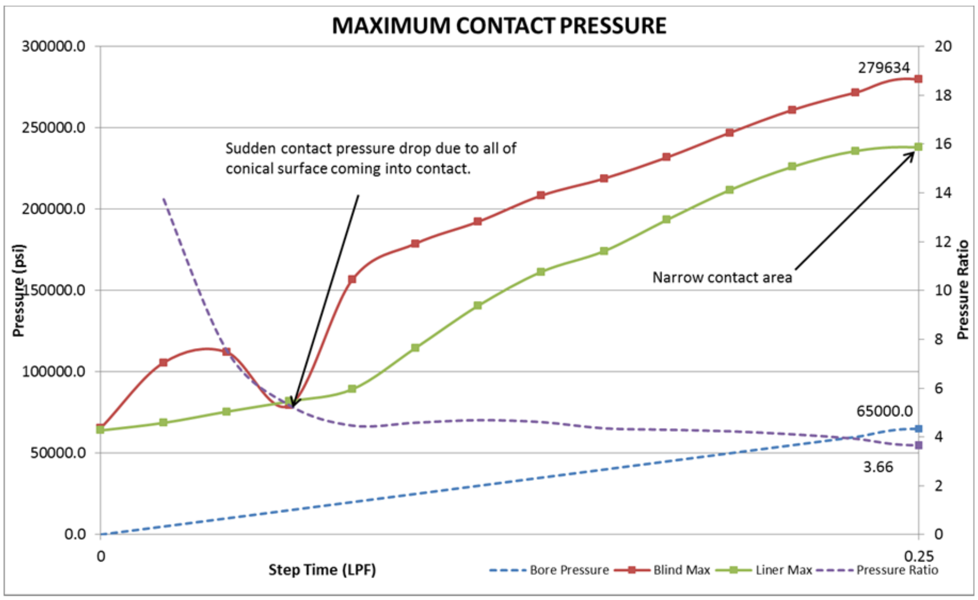


**Figure 3-5: Seal contact stress plot (0-65,000 psi; partial hydrotest)**

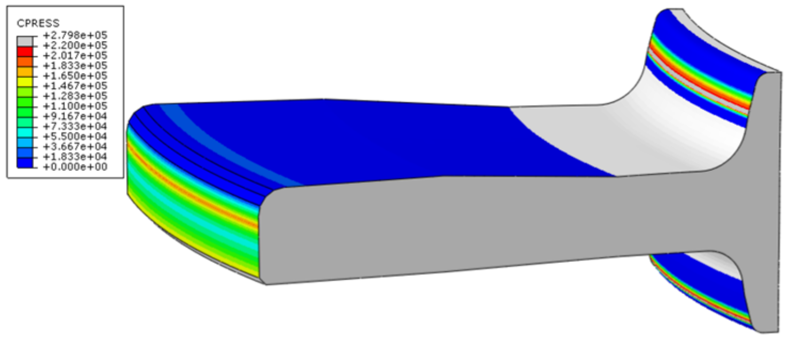


**Figure 3-6: Seal contact stress (@65,000 psi bore pressure)**

Looking at Figure 3-7, the blind seat is exhibiting localised plastic strain (0.004) forming on the seat area due to the blind rotating inwards. This generates negative hoop stress, coupled with the very high dominating negative radial stresses (Figure 3-6) from the seal ring, there is enough primary stress differential to generate a high von Mises stress and hence plastic yield.

Regarding the liner, the bore pressure forces the liner to expand radially, this creates positive hoop stress (opposite to the blind seat). Couple this with the negative radial contact stress from the seal ring there is a substantial differential of primary stresses to generate von Mises stress that is high enough to create plastic strain, which reaches 0.009.

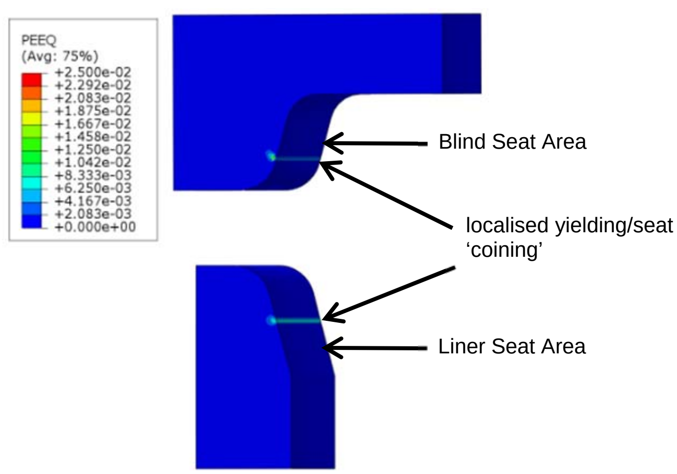


**Figure 3-7: Seat plastic yield (@65,000 psi)**

To conclude, the high seal ring CPRESS values combined with the seat displacements are causing yielding of the surface of the seal interface and both seat areas. Therefore a revised design is required to spread contact stress and reduce peak stresses at the interfaces.

## 3.5 Optimised Seal Ring Model

To reduce the contact pressures being developed using the conical type sealing interface it was deemed necessary to use a novel type of interface. Figure 3-8 shows the 'profiled' type interface which was developed so that the seal ring has greater flexibility due to internal loadings and the contact area would adjust in a non-linear fashion. Many simulations were run due to various complex issues arising; from this analysed data, the profiles were developed iteratively to perform the following actions:

- On the blind side during pressurisation, contact area will progressively increase to limit excessive contact pressure, hence decreasing the plastic strain.
- On the liner side, the contact area will decrease during pressurisation. Thus the liner swells radially outwards. The liner seat deflects 11 times more than the blind side, hence the reason why less sealing area is required.

The seal ring loadings on this model have also been amended. In section 2.4 it is highlighted that pressure penetration can be used to accurately position the loading up to the contact stress. It was discovered whilst modelling with Abaqus/Standard 6.12-3, that the pressure penetration could effectively propagate the loading toward the contact stress, however it could not regress the loading. This in turn would result in incorrect contact pressure results during loading on the liner side, as the contacts in this region shift outwards. To overcome this issue the loading on the liner side was returned to a static position. The results for a hydrotest are shown below in Figure 3-8 and Figure 3-9.

The maximum contact stress reaches 160,000 psi (Figure 3-8 and Figure 3-9) at 65,000 psi bore pressure. When compared to the proposed seal ring this reaches 280,000 psi (Figure 3-5). This is 43% lower which is a significant drop. This has been the main aim of the project; to keep the contact pressure ratio above the acceptable level, whilst not being detrimental to the interface.

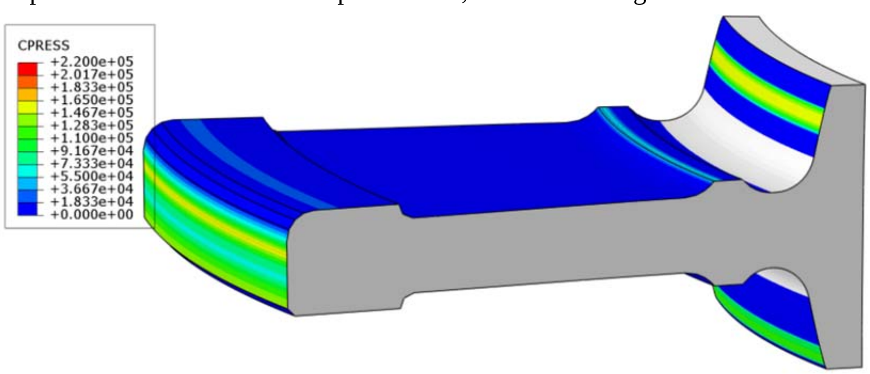


**Figure 3-8: optimised seal contact stress (@65,000 psi; full hydrotest)**

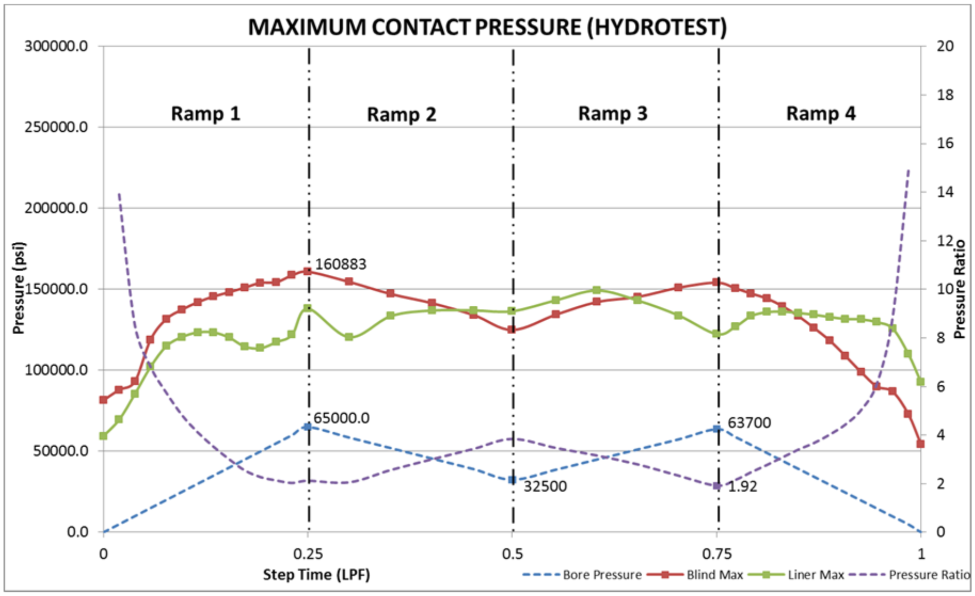


**Figure 3-9: Seal contact stress plot (full hydrotest)**

The initial contact pressures for both the blind and liner side are different at the end of the cycle (Figure 3-9). This is due to the reactor seat movements (uncontrollable) and pressure loads involved generating rib yielding. At 65,000 psi, the max rib plastic strain value is 0.02128, then at 0 psi this increases to 0.02582. This shows that the material is work hardening during a hydrotest. This yielding would keep summating on subsequent hydrotests and therefore would raise a concern of failure due to fatigue. This being the case, it was deemed necessary to limit a seal ring to one hydrotest only, then use a second for operation.

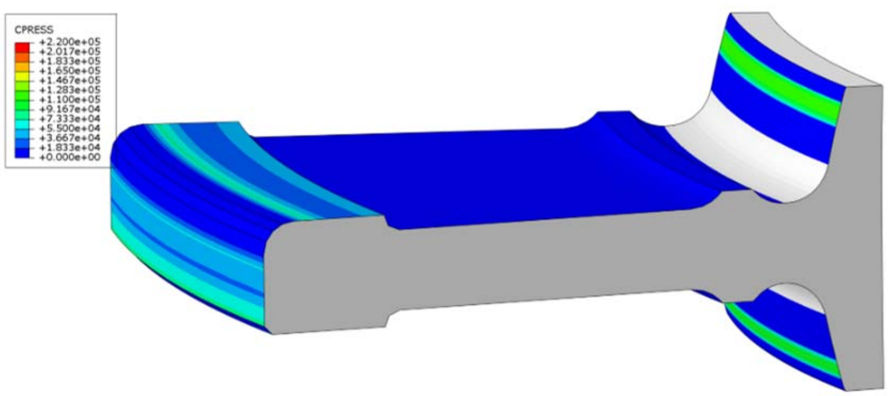


**Figure 3-10: optimised seal contact stress (@32,500 psi/500°F)**

When this seal ring was simulated thermo-mechanically the maximum predicted stress (Figure 3-10 and Figure 3-11) being exhibited by this seal is 126,000 psi, which results in a very acceptable pressure ratio of 3.48. The maximum contact stresses have a very similar trend on the 2nd cycle, this shows that the profiled interface is performing well and not creating any pressure spikes.

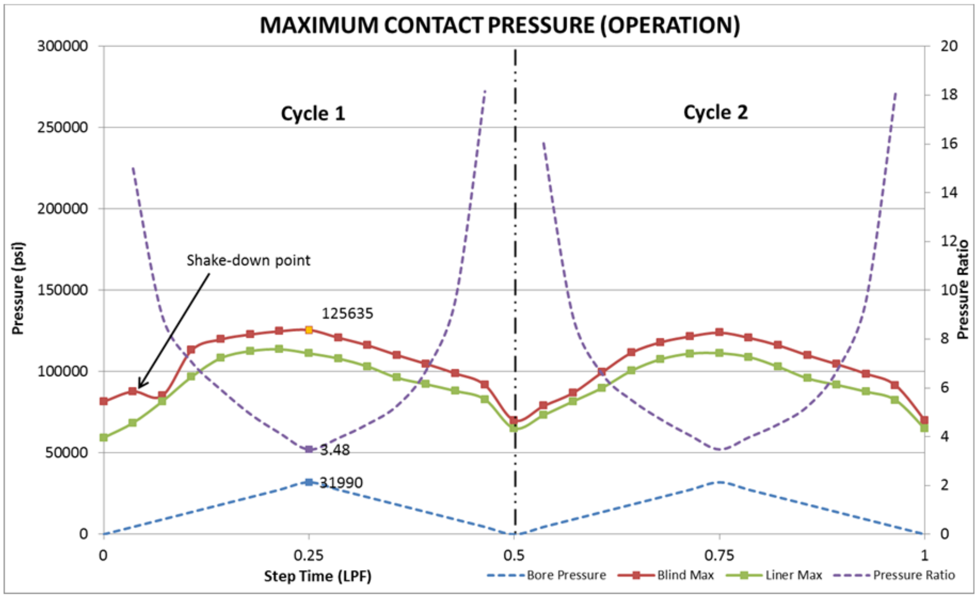


**Figure 3-11: Seal contact stress plot (operational run)**

The seal undergoes 'shake-down', which results in different contact pressures at make-up when compared to zero bore pressure after make-up. This phenomenon occurs due to friction about the seal rib which forces the seal ring inwards during the bolt tensioning stage. Varied frictional coefficients have been tested to verify this issue. 'Shake-down' only occurs during the first pressurisation cycle, which would suggest an initial pressure loading should be performed before the vessel can be used.

## 3.6 Current problem

When looking at solid contacting surfaces within Abaqus, it is possible to apply a pressure field up to the contact from a designated start point. As the contact shifts away (reduces the critical contact pressure) from the specified pressure penetration start point; whether this is due to some input such as force or displacement, the pressure field will propagate forwards (away from the specified starting point) between the master and slave surfaces. When analysing metallic seal rings (as in Section 2) this can be highly beneficial and give a more 'realistic solution' by relieving seating stresses when higher pressures are induced, where the back end of seal will become exposed to the pressure loading.

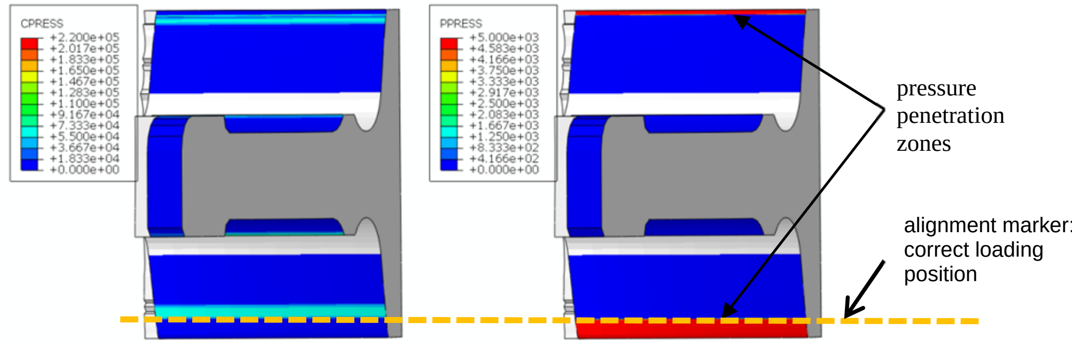


**Figure 3-12: Pressure penetration (@5,000 psi)**

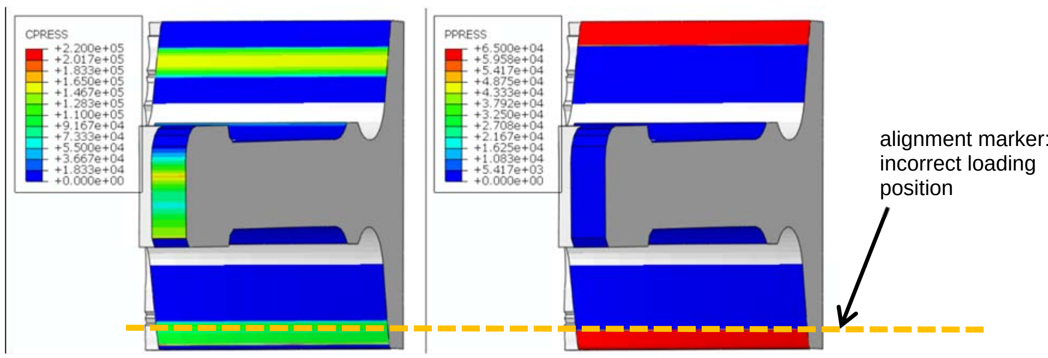


**Figure 3-13: Pressure penetration (@65,000 psi)**

The current limitations of the software are that once the pressure field has been exposed to the element faces, they cannot back propagate i.e. once the pressure penetration surfaces have been exposed, they remain active even though the 'critical contact pressure' has been re-satisfied. This could be detrimental to final results, as it could be applying unnecessary loadings to the sealing surface. The task has been to create a User Subroutine (USR) written in FORTRAN which can handle both progressive and regressive propagation of pressure field application.

Figure 3-12 and Figure 3-13 show a current example where the back propagation would be necessary. This is the investigation from Section 2. It is apparent that incorrect loading (Figure 3-13) is observed on regressive contacts when using the Abaqus pressure penetration module.

### 3.7 Solution and method

A subroutine has been designed which propagates the pressure loading on one axis, as the seal rings have contacts which always lay on one plane in space, this solution was sufficient. Acquiring and inputting data using Abaqus [3] can be done by using 'URDFIL' to extract nodal and element data; 'DLOAD' to input Loading parameters then 'UVARM' for a visual representation in the Complete Abaqus Environment (CAE).

## 3.8 Results

The results shown here are for a simplified four point contact/group model, which mimics a four contact seal ring. The assembly is a section of a cylindrical design which has a slight clearance between the two separate components, where the pressure propagates up to a ‘displacement generated’ point; this has been modelled using a Cylindrical Coordinate System (CCS). Results are as shown in Figure 3-14.

As can be seen from the ‘UVARM’ contour plots in (Figure 3-14), the elements are being exposed/concealed to loadings as the CPRESS shifts due to the central column displacing. Where the red elements are at full pressure the green elements are the ‘birth elements’ (half loading) to aid model convergence. This is performed by creating a history report then comparing this to new pressure locations.

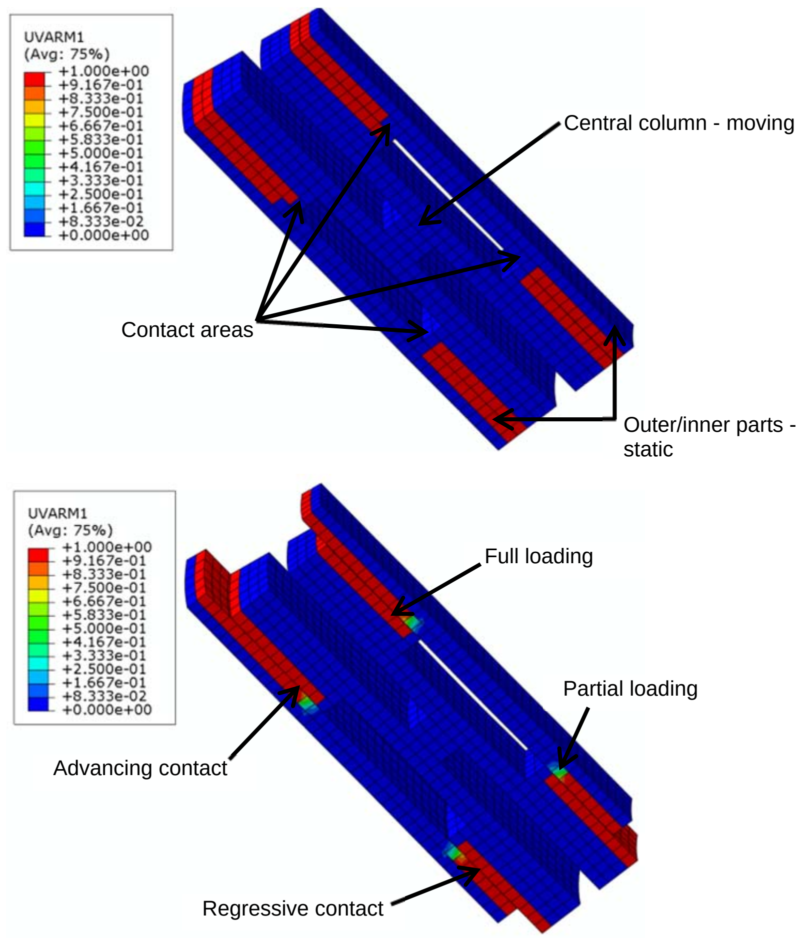


**Figure 3-14: USR pressure penetration (step 0 (top), step 30 (bottom)**

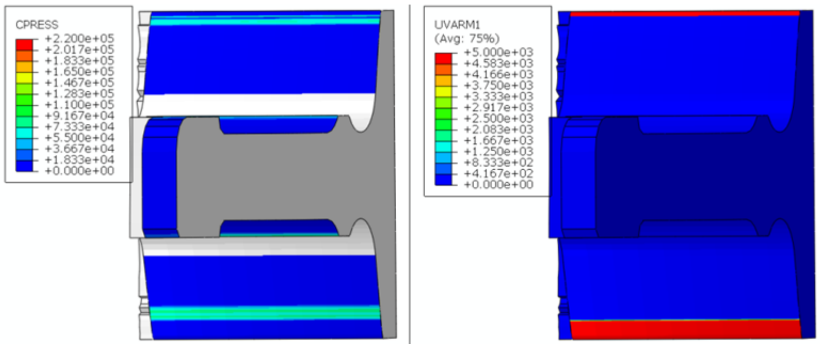

**Figure 3-15: USR pressure penetration (@5,000 psi)**

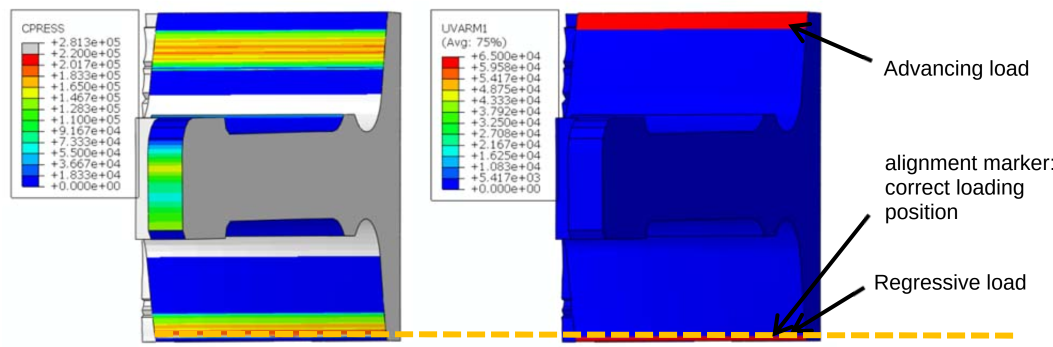


**Figure 3-16: USR pressure penetration (@65,000 psi)**

After extensive testing of the code, the subroutine was applied to the seal from Section 2.5; the results are shown in Figure 3-15 and Figure 3-16.

The result has proved that the subroutine is successful, where the contact pressures have also changed due to the correct real-time positioning of the loads. This code can now be applied to a four point contact seal ring which is the next stage of the work.

## 4. Overall conclusions and further work

Vector Technology Group have achieved two large investigations under one project, which are the pressure vessel seal ring analysis and optimisation, and the pressure penetration modelling by creating a novel USR. Applying the subroutine on future seal ring work would remove the time consuming iterative process currently required to predict where the pressure loading is applied, whilst also gaining greater accuracy when modelling such systems.

The profiled design has proved that it can control, in a non-linear fashion, contact pressure variation when bore pressure is applied. This design is therefore suitable for bespoke cases where unsymmetrical seat movements are observed.

The following can be deduced for this investigation:

- Detrimental seat deformations during hydrotest were being generated from the original conical seal design. The final profiled design reduced maximum seat plastic strain by:
    - Liner = 87%
    - Blind = 99.99%
- During hydrotest the yield forming in the seal ring was increasing during the test i.e. work hardening. This being the case only one seal can be used if a hydrotest is performed on it. The yield however is not detrimental to sealing efficiency.
- During a thermo-mechanical cycle, no work hardening is taking place and the contact pressures and their sealing positions are within specification.
- The pressure penetration module with Abaqus was providing incorrect liner side CPRESS predictions, therefore manual intervention was required to give more accurate results. Future work is necessary to achieve a more automated solution.

Further work could include the following:

- The ‘profiled’ seal ring interface design could be implemented on a four-point seal ring, which would aid high contact stress problems at extreme pressures; couple this with the pressure penetration subroutine and the results will be more accurate and hence give Vector more confidence in the results.
- The USR to use an element search routine which would allow any surface contour to be subjected to pressure penetration. Coupling both Abaqus and the USR together will provide Vector with a very powerful analysis tool for future FEA seal ring modelling.

This project has been highly successful, where novel techniques have been implemented to solve complex issues. Also further work has been recognised which can re-enforce future modelling issues.

## 5. References


1. Araujo M.C, “Non-linear kinematic hardening model for multiaxial cyclic plasticity,” Thesis, Department of Civil and Enviromental Engineering., Louisiana University, USA, 2002.
2. W. C. Young, *Roark’s Formulas for Stress & Strain*, 8th ed. Mc Graw Hill, 2012, pp. 621–698.
3. Abaqus Users Manual, Version 6.12-3, Dassault Systèmes Simulia Corp., Providence, RI.